ELSEVIER

Chemical Geology 224 (2005) 69–81

CHEMICAL GEOLOGY
INCLUDING
ISOTOPE GEOSCIENCE

www.elsevier.com/locate/chemgeo

# Tide-influenced acidic hydrothermal system offshore NE Taiwan

Chen-Tung Arthur Chen [a,*], Zhigang Zeng [b], Fu-Wen Kuo [a], Tsanyao Frank Yang [c], Bing-Jye Wang [a], Yueh-Yuan Tu [d]

[a] *Institute of Marine Geology and Chemistry, National Sun Yat-Sen University, Kaohsiung 804, Taiwan, ROC*
[b] *Institute of Oceanology, Chinese Academy of Sciences, Qingdao, PR China*
[c] *National Taiwan University, Taipei, Taiwan, ROC*
[d] *Taiwan Power Company, Taipei, Taiwan, ROC*

Received 27 November 2004; accepted 4 July 2005

**Abstract**

Elemental sulfur and hydrogen sulfide emitted offshore of northeastern Taiwan known to local fishermen for generations, but never studied until recently, are found to have originated from a cluster of shallow (<30 m depth) hydrothermal vents. Among the mounds is a massive 6 m high chimney with a diameter of 4 m at the base composed of almost pure sulfur and discharging hydrothermal fluid containing sulfur particles. The sulfur in the chimney has a $\delta^{34}S = 1.1‰$ that is isotopically lighter than seawater. A yellow smoker at shallow depths with such characteristics has never been reported on anywhere else in the world. Gas discharges from these vents are dominated by $CO_2$ (>92%) with small amounts of $H_2S$. Helium isotopic ratios 7.5 times that of air indicate that these gases originate from the mantle. High temperature hydrothermal fluids have measured temperatures of 78–116 °C and pH (25 °C) values as low as 1.52, likely the lowest to be found in world records. Low temperature vents (30–65 °C) have higher pH values. Continuous temperature records from one vent show a close correlation with diurnal tides, suggesting rapid circulation of the hydrothermal fluids.


*Keywords:* Hydrothermal vents; Taiwan; Yellow smoker; Acidity; Tides; Phase separation

## 1. Introduction

The presence of hot springs in Taiwan has been well known for several centuries. As far back as the 17th century early settlers used spring waters of the Tatun volcanic group in northern Taiwan for bathing and curing skin diseases. This volcanic group is the site of the last volcanic activity in northern Taiwan (Fig. 1) which ceased ca. 200,000 years ago (Chen, 2000). However, many high-temperature solfataras and springs, some even boiling, are scattered in the area. The subsurface thermal water is acid sulfate chloride, with temperatures ranging between 120 and 293 °C (Chen, 1996). There are more than 200 thermal springs in Taiwan (the mountainous island of 36,000 $km^2$), including some bicarbonate springs on the Ilan Plain (Fig. 1). Given these facts, what should have been expected long ago is that hot springs exist offshore too. However, not until 1999 were offshore thermal springs documented and studied (Chen et al., 2005). These springs are located in an active hydrothermal vent field of about 0.5 $km^2$ in area within 1 km east of Kueishantao islet, at 121°55′E, 24°50′N, near the southern end of the Okinawa Trough (Fig. 1).

* Corresponding author. Fax: +886 7 525 5346.
*E-mail address:* ctchen@mail.nsysu.edu.tw (C.-T.A. Chen).

0009-2541/$ - see front matter © 2005 Elsevier B.V. All rights reserved.
doi:10.1016/j.chemgeo.2005.07.022

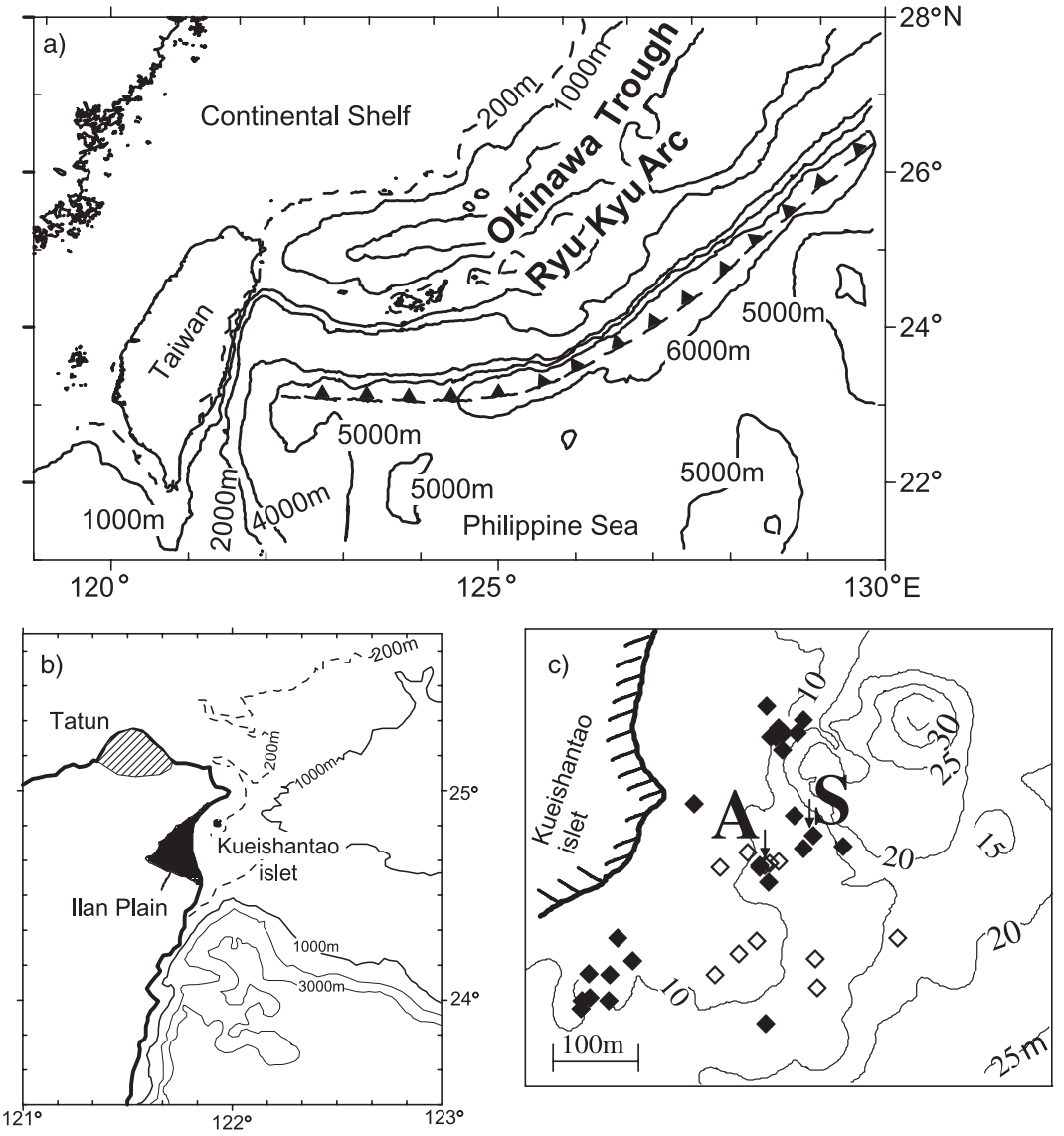


Fig. 1. Map showing (a) Taiwan and Okinawa Trough, (b) the tectonic setting of Kueishantao islet and (c) the location of vents. The arrows point to vents A and S. Solid diamonds indicate high temperature vents and open diamonds indicate low temperature vents.

The Okinawa Trough is the backarc basin of the Ryukyu subduction zone which is still extending westward through the development of an E–W trending graben caused by the subduction of the Philippine Sea Plate beneath the Eurasian Plate. The collision system, with its intensive tectonic activity, extends about 1000 km from southwestern Kyushu in Japan to northeastern Taiwan (Wang et al., 2002). Active tectonism has caused many earthquakes, including the Richter scale magnitude 7.3 Chi-Chi earthquake on 21 September 1999, that killed several thousand people in Taiwan. Many volcanic islands dot the region, and one of the youngest of these is Kueishantao islet where the last major eruption occurred ca. 7000 years ago (Chen et al., 2001).

The Okinawa Trough shoals and narrows down westwards near Taiwan to the east of the Ilan Plain. Two seismic belts are situated near the axial center of the southern Okinawa Trough. The northern seismic belt extends to Kueishantao islet off the Ilan Plain. Although seismic data suggest that the southern belt stops about 20 km short of Kueishantao islet, geophysical data indicate that the graben extends farther westwards (Lee et al., 1980; Wang et al., 2002).

## 2. Study area and methods

An estimated cluster of more than 30 vents were observed at depths of about 10–30 m. These vents were identified by scuba divers and their positions located by GPS (Fig. 1). PVC tubes were inserted into selected vents. Vent gases were collected in Giggenbach bottles filled with an alkaline solution (Giggenbach, 1975; Fischer et al., 1996; Fischer and Hilton, 2003; Taran et al., 2002). The non-dissolved gases, including $H_2$, He, $N_2$, $O_2$, Ar, $CH_4$ and CO were measured in a gas chromatograph (GC). Gases dissolved in the alkaline solution, i.e., $CO_2$, HCl, $H_2S$ and $SO_2$, were titrated and analysed with an Ion Chromatograph (IC). Analytical procedures are described by Lee and Yang (2005).

Temperatures were measured with a thermocouple inserted into the vents. In addition, continuous temperature recorders (Pace Scientific Inc. XR 440 Pocket Logger with Mvt-11 thermocouple) were attached at our primary sample vent (hereafter referred to as Station A or St. A) and in the seafloor 1 m away from that vent. Flow rates were measured with a Hydro Bios Model 438-110 Digital Flow Meter. A Guildline salinometer (Autosal 8400B) was used to measure conductivity which was then converted to salinity. pH values were determined using a Radiometer PHM-85 pH meter at 25 °C, while major ions were measured using a Dionex DX-120 Ion Chromatograph. Values for nitrate as well as nitrite were obtained by following the pink azo dye method with a flow injection analyzer. Phosphate was determined using the molybdenum blue method, and $SiO_2$ measured employing the silicomolybdenum blue method, also with a flow injection analyzer. Fe, Mn and Al were measured using the Ferrozine spectrophotometric method, Inductive Coupled Plasma (ICP) and the fluorescence methods, respectively. Isotopes were determined with a mass-spectrometer. $^3He/^4He$ and $^4He/^{20}Ne$ ratios were measured with a Micromass 5400 noble-gas mass spectrometer with dual collectors. Air was routinely run as a standard for calibration. In general, the total errors of the ratios are less than 2% and 5% for $^3He/^4He$ and $^4He/^{20}Ne$, respectively. Details of analytical procedures are given in Yang (2000) and Yang et al. (2003).

## 3. Results and discussion

### 3.1. Sulfur mounds and chimney

Hydrothermal fluids are mainly discharged out of edifices and yellow mounds about 2 m high and 2–3 m wide at the base. Almost pure sulfur ($99.64 \pm 0.21\%$, $n = 5$) with some α-phase crystals and trace amounts of pyrite comprise these mounds. Apart from sulfur, large amounts of gypsum and anhydrite are scattered over the seabed.

A large yellow smoker, about 6 m high and 4 m across at the base and sitting at a water depth of 20 m, was discovered on 12 August 2000. Fourteen samples of native sulfur were analysed for S isotopic compositions. The $\delta^{34}S$ ranges of −0.5‰ to 2.0‰ (Table 1; average: 1.1‰) are isotopically lighter than seawater. At this stage it is not clear whether the sulfur originated from the reduction of sulfate in seawater, fractionation of hydrothermal fluids or magma/mantle degassing. The narrow $\delta^{34}S$ range, however, suggests a relatively simple source for the native sulfur.

The $\delta^{34}S$ values of the seafloor native sulfur chimney off Kueishantao islet are lighter than those of the Jade hydrothermal field in the Okinawa Trough but heavier than those of the Lau basin (Table 2). This is our first indication that the sulfur sources which formed the native sulfur in Kueishantao islet, Jade and the Lau basin must be different.

The sulfur isotopic composition of native sulfur in the hydrothermal field off Kueishantao islet are distinctly different from the $\delta^{34}S$ of sulfides (Fig. 2) found in back-arc settings such as the Okinawa Trough, Lau basin and Mariana Trough but are analogous to values in non-sediment-covered Mid-Ocean

Table 1
Sulfur isotopic compositions of native sulfur from the chimney off Kueishantao islet

| Sample no. | $\delta^{34}S_{CDT}$ (‰) |
|---|---|
| GSD-3-1 | 0.5 |
| GSD-3-2 | 1.5 |
| GSD-3-3 | 1.7 |
| GSD-3-4 | −0.6 |
| GSD-3-5 | 1.7 |
| GSD-3-6 | 1.5 |
| GSD-3-7 | 0.7 |
| GSD-3-8 | 1.6 |
| GSD-3-9 | 1.8 |
| GSD-3-10 | 1.7 |
| GSD-3-11 | 1.3 |
| GSD-3-12 | 2.0 |
| GSD-3-13 | −0.5 |
| GSD-3-14 | 1.5 |

Analysed by: Institute of Mineral Deposits, Chinese Academy of Geological Sciences, Bai Ruimei, Luo Xurong.
Method: After being fritted with carbonate-ZnO, $SO_2$ gas was generated following the method of $V_2O_5$ oxidation.
Instrument: Finnigan MAT Delta S.
Precision: ±0.2‰.
Repeat determination for each sample: 4–5.

Table 2
Comparison of the sulfur isotopic values of the native sulfur samples off Kueishantao islet with other hydrothermal fields

| Hydrothermal field | $\delta^{34}S_{CDT}$‰ | Data source |
|---|---|---|
| Kueishantao | −0.5~2.0 (mean: 1.1) | This study |
| Jade | 8.2 | Zeng et al., 2000a |
| Jade | 6.6~11.2 | Marumo and Hattori, 1999 |
| Lau basin | −4.8~−2.4 (mean: −3.4) | Herzig et al., 1998a |

Ridge (MOR) hydrothermal fields e.g., Axial Seamount, Southern Juan de Fuca Ridge, EPR, Snake Pit and Broken Spur. Fig. 2 also shows that the range of sulfur isotopic compositions is significantly narrower in the hydrothermal field off Kueishantao islet than in the sediment-covered MOR sites of the Guaymas basin, Middle Valley and Escanaba Trough, suggesting that sulfur of the chimney off Kueishantao islet comes from a single source.

Turning to the source of the sulfur of the seafloor native sulfur chimney, although andesite made up the basement of this underwater chimney, the sulfur that formed the chimney could clearly not have been from Kueishantao andesite. According to two reports, one by Ueda and Sakai (1984) and the other by Woodhead et al. (1987), the $^{34}S$ values of the island-arc lava (andesite and rhyolite) are between +5‰ and +7‰, values, which are significantly higher than that of the sulfur chimney off Kueishantao islet. Compared with the $^{34}S$ values of the Mid-Ocean Ridge basalts ($\delta^{34}S = +0.1 \pm 0.5$‰; Sakai et al., 1984), those of the native sulfur chimney off Kueishantao islet are analogous to those of MORBs (Table 3), which provides strong support for the argument that the sulfur of the chimney was from the deep mantle and that the sulfur isotopic characteristics originated from magma degassing.

The large underwater chimney off Kueishantao islet was destroyed by Typhoon Bilis on 22 August 2000.

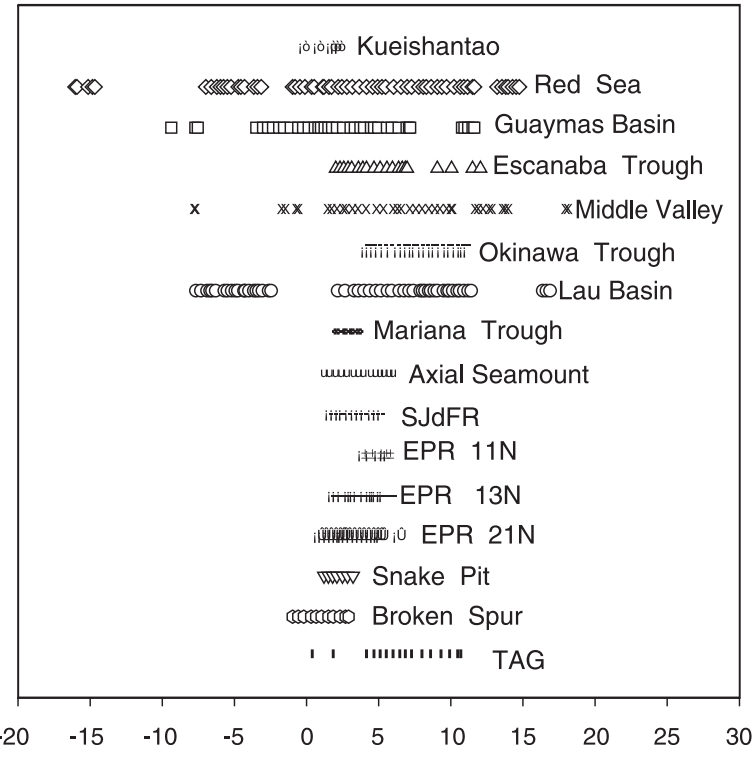


Fig. 2. Comparison of the sulfur isotopic values of the native sulfur samples off Kueishantao islet with those of sulfides from other hydrothermal fields. Data sources: Kueishantao (this study); Red Sea (Zierenberg and Shanks, 1988; Blum and Puchelt, 1991); Guaymas basin (Shanks and Niemitz, 1982; Koski et al., 1985; Peter and Shanks, 1992); Escanaba Trough (Koski et al., 1988; Zierenberg et al., 1993); Middle Valley (Duckworth et al., 1994; Stuart et al., 1994; Zierenberg, 1994; Goodfellow and Franklin, 1993); Okinawa Trough (Halbach et al., 1989; Zeng et al., 2000a); Lau basin (Herzig et al., 1998a); Mariana Trough (Kusakabe et al., 1990); Axial Seamount (Hannington and Scott, 1988); SJdFR (Shanks and Seyfried, 1987); EPR 11°N (Bluth and Ohmoto, 1988); EPR 13°N (Bluth and Ohmoto, 1988); EPR 21°N (Stuart et al., 1994; Hekinian et al., 1980; Arnold and Sheppard, 1981; Zierenberg et al., 1984; Woodruff and Shanks, 1988; Alt, 1988; Kerridge et al., 1983); Snake Pit (Stuart et al., 1994; Kase et al., 1990); Broken Spur (Knott et al., 1998); TAG (Stuart et al., 1994; Knott et al., 1998; Chiba et al., 1998; Herzig et al., 1998b; Gemmell and Sharpe, 1998; Zeng et al., 2000b).

Table 3
Comparison of the sulfur isotopic values of the native sulfur samples off Kueishantao islet with those endmembers

| MORB | Kueishantao | Island-arc volcanic rock (andesite and rhyolite) | Seawater |
|---|---|---|---|
| 0.1 ± 0.5 | −0.5–2.0 (mean: 1.1) | 5–7 | 20.9 |

Data from Sakai et al., 1984, Ueda and Sakai, 1984, Woodhead et al., 1987, Rees et al., 1978 and this work.

The strong wave actions generated by the typhoon very likely caused the demise of the chimney and scattering of debris.

### 3.2. Gas phase

The dry gas compositions of the bubbles of the hydrothermal fluids (Table 4) are dominated by $CO_2$ (>92%) but with small amounts of $H_2S$ (0.9–8.4%) and other trace gases. This is the typical composition of low-temperature (<400 °C) fumarolic and hydrothermal gases, i.e., these gases exhibit low total sulfur contents but high $H_2S/SO_2$ and $CO_2/S_{total}$ ratios (Fig. 3). Besides this, the consistently high helium isotopic ratios of 7.4–7.6 times that of air strongly indicate that more than 93% of these gases are derived from a mantle component, reconfirming conclusions from the $\delta^{34}S$ results that they are primarily of magmatic origin.

In contrast to sulfate sulfur in melts, the outgassing of $H_2S$ can cause $H_2S$ sulfur to be significantly depleted in $^{34}S$ (Zheng et al., 1996), which can bring about a negative $\delta^{34}S$ value for native sulfur. Contrast this with sulfide sulfur in melts, where the outgassing of $SO_2$ can cause $SO_2$–sulfur to be significantly enriched in $^{34}S$ (Zheng et al., 1996), which can result in a positive $\delta^{34}S$ value for native sulfur. Based on a simple two-endmember mixing model, more than 90% of the sulfur of the native sulfur chimney off Kueishantao islet was from the deep mantle, whereas the amount of sulfur from seawater was negligible. This means that the magma under Kueishantao islet is still active and is still degassing sulfur and other gases from the mantle. The circulation period of the submarine hydrothermal system above the magma is very short, thus the vent fluids are mainly composed of little-changed seawater, as discussed below.

### 3.3. Hydrothermal fluids

Earlier attempts, during this study, to obtain long-term temperature records of the fluids coming out of the high temperature edifices and vents were unsuccessful because the thermocouples with stainless steel casting either corroded away within days or could not be retrieved. Apart from these problems, it was also physically impossible to leave a thermocouple in the yellow chimney since it was growing about 30 cm a day. For these reasons, we chose to record long-term temperatures at St. A, which has a lower temperature and less corrosive fluids.

The vents discharge waters as hot as 116 °C (St. S) and as acidic as pH (25 °C) 1.517. This level of acidity

Table 4
Dry gas compositions[a] of Kueishantao submarine hot springs

| Sample locations | Temp. (°C) | $[^3He/^4He]_c$[b] | He | Ar | $N_2$ | CO | $CH_4$ | $H_2$ | $O_2$ | HCl | $SO_2$ | $H_2S$ | $CO_2$ | Data[c] source |
|---|---|---|---|---|---|---|---|---|---|---|---|---|---|---|
| *Kueishantao (KST)* | | | | | | | | | | | | | | |
| 030622-GSD-VAJ | 55 | 7.54 | 0.028 | 0.009 | 0.871 | 0.0004 | b.d.l. | 0.114 | 0.195 | 0.028 | 0.271 | 20.4 | 978 | 1 |
| 030622-GSD-VA | 48 | 7.54 | 0.025 | 0.025 | 2.231 | 0.0008 | 0.335 | 0.0007 | 0.032 | 0.049 | 0.226 | 21.0 | 976 | 1 |
| 030814-GSD-VA | 56 | 7.39 | 0.015 | 0.001 | 0.108 | 0.00008 | 0.035 | 0.021 | 0.011 | 0.023 | 0.073 | 8.46 | 992 | 1 |
| 030814-GSD-VAK | 107 | 7.53 | 0.007 | 0.0004 | 0.043 | 0.00001 | 0.007 | 0.003 | 0.007 | 0.023 | 0.009 | 12.6 | 987 | 1 |
| 030815-GSD-VAL | 78 | 7.58 | 0.005 | 0.0002 | 0.024 | 0.00001 | 0.030 | 0.002 | 0.002 | 0.030 | 0.051 | 84.0 | 916 | 1 |
| 030815-GSD-VAM | 95 | 7.46 | 0.005 | n.d. | n.d. | n.d. | n.d. | n.d. | n.d. | n.d. | n.d. | n.d. | n.d. | 1 |
| *Other volcanoes in the world* | | | | | | | | | | | | | | |
| Tankkuban Parhu, Indonesia | 94 | n.d. | 0.004 | n.d. | 7.60 | n.d. | 0.03 | 4.81 | n.d. | 1.75 | 25.4 | 371 | 550 | 2 |
| White Island, New Zealand | 111 | n.d. | 0.002 | 0.03 | 9.80 | n.d. | 8.90 | 0.20 | n.d. | 3.60 | 4.53 | 170 | 808 | 3 |
| Papandayan, Lower Vent, Indonesia | 282 | n.d. | 0.005 | n.d. | 10.4 | 0.002 | 0.01 | 2.94 | 0.67 | 28.0 | 3.86 | 18.2 | 691 | 2 |
| Mt. Usu, Japan | 690 | n.d. | n.d. | n.d. | 16.0 | 0.08 | 0.90 | 294 | n.d. | 68.0 | 52.2 | 29.3 | 575 | 3 |
| Merapi, Gendol, Indonesia | 803 | n.d. | 0.004 | 4.29 | 319 | 1.08 | n.d. | 44.3 | 1.59 | 53.8 | 95.4 | 13.0 | 489 | 2 |

[a] Except for helium isotopic composition, all gas compositions shown as the unit of millimoles ($10^{-3}$ mole) per mole.
[b] Helium isotopic ratios normalized to atmospheric air ratio ($^3He/^4He = 1.4 \times 10^{-6}$) after correction of air contamination (Poreda and Craig, 1989); data from Yang et al. (in preparation).
[c] Data from (1) this study; (2) Giggenbach et al. (2001); (3) Giggenbach and Matsuo (1991).

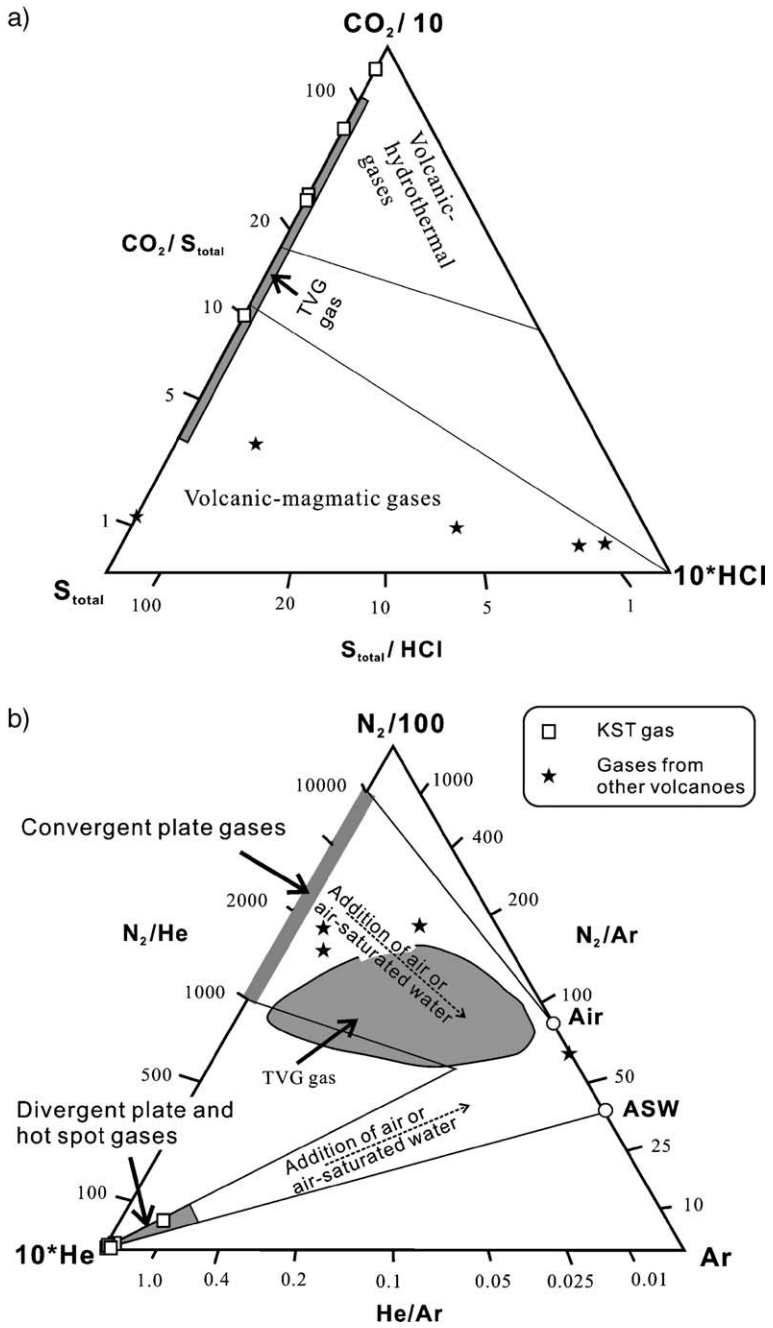


Fig. 3. Three-component plots of the Kueishantao (KST) hot spring gases. (A) $CO_2$–S–HCl plot, most KST samples exhibit a high $S_{total}/HCl$ and $CO_2/S_{total}$ ratio, which are similar with those of Tatun Volcano Group (TVG) but show distinct deviations from the gases from other active volcanoes, indicative of a volcanic–hydrothermal origin. (B) $N_2$–He–Ar plot, KST samples fall in the corner of compositions of divergent plate and hot spot gases, which are significantly different from those from TVG and convergent plate gases. Gas boundary followed Delmelle and Stix (2000). TVG gas data are from Yang et al. (2003) and Lee et al. (2005); other data are from Table 4. Note that $N_2$ and Ar data are plotted after oxygen correction assuming that all oxygen comes from air contamination.

is perhaps the lowest ever reported for any hydrothermal vent in the oceans of the world (Gamo et al., 1997). The pH levels generally decrease with higher temperatures (Fig. 4). Surprising, however, trace metal concentrations are relatively low even with such low levels of pH. The dissolved oxygen concentrations are also low, whereas the sulfide concentrations are high. The ranges of the chemical parameters for the high temperature

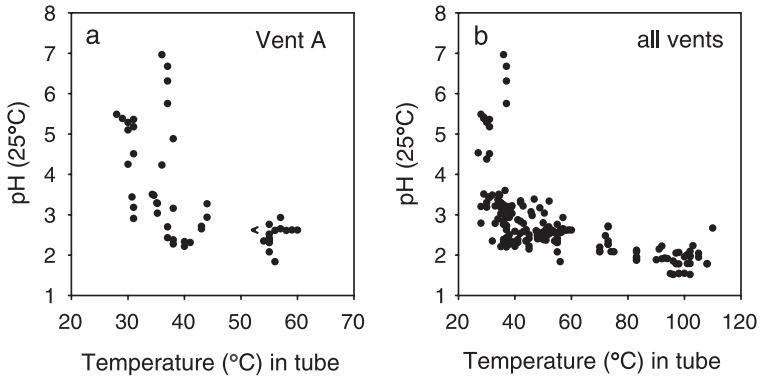


Fig. 4. pH values (25 °C) plotted vs. temperatures of the hydrothermal fluids at (a) vent St. A and (b) all vents, as measured in the collection tubes.

(78–116 °C; mean 106 ± 9 °C) and low temperature (30–65 °C; mean 50.7 ± 8 °C) fields, respectively, are given in Tables 5 and 6 (original digital data available from CTA Chen). On account of the high salinity (>30) and similar major ion ratios as seawater, it seems reasonable to conclude that the hydrothermal fluids must have originated from the seawater. It is important to note that salinity is defined here in terms of relative conductivity without a unit, a definition which is in line with practices in oceanography. Any inhomogeneity in the composition of a seawater sample affects the relationship between seawater components and conductivity (e.g. Chen and Gordon, 1979). Because $H^+$ has a much higher specific conductivity than other seawater

Table 5
Chemical composition of high temperature hydrothermal fluids near Kueishantao islet

| | Range | Mean | No. of observations |
|---|---|---|---|
| T°C | 78~116 | 106 ± 9.16 | 115 |
| Salinity* | 31.3~36.5 | 33.9 ± 1.26 | 116 |
| Salinity** | 30.3~34.8 | 32.5 ± 1.1 | 96 |
| pH (25 °C) | 1.52~6.32 | 2.49 ± 0.72 | 116 |
| Dissolved oxygen (μM) | <0.3~141 | 10 ± 29.7 | 114 |
| $NO_3$ (μM) | 0.30~12.3 | 3.04 ± 4.01 | 16 |
| $NO_2$ (μM) | 0.01~0.17 | 0.032 ± 0.039 | 20 |
| $NH_3$ (μM) | <0.71~714 | 74 ± 181 | 20 |
| $PO_4$ (μM) | <0.05~2.67 | 0.65 ± 0.78 | 15 |
| $SiO_2$ (μM) | 4.94~1052 | 269 ± 270 | 116 |
| Chlorophyll a (μg/l) | <0.01~0.55 | 0.06 ± 0.12 | 18 |
| $CH_4$ (μM) | 1.3–744 | 93 ± 184 | 20 |
| $S^{-2}$ (μM) | 0.03~19 | 3.4 ± 6.3 | 20 |
| Cl (mM) | 479~557 | 509 ± 16.8 | 96 |
| $SO_4$ (mM) | 24.5~30.4 | 26.8 ± 1.32 | 96 |
| Na (mM) | 391~485 | 433 ± 20.8 | 96 |
| K (mM) | 8.43~9.9 | 9.16 ± 0.27 | 96 |
| Mg (mM) | 43.9~54.4 | 48.7 ± 2.25 | 96 |
| Ca (mM) | 8.49~10.8 | 9.43 ± 0.50 | 96 |
| Al (μM) | 0.4~1009 | 237 ± 294 | 111 |
| Fe (μM) | 0.319~177 | 22.3 ± 32.8 | 113 |
| Mn (μM) | <0.008~23.2 | 1.31 ± 2.43 | 113 |
| Cu (nM) | <0.2~3561 | 218 ± 862 | 17 |
| Zn (nM) | <1~1399 | 232 ± 407 | 17 |
| Cd (nM) | <0.01~4.70 | 1.30 ± 1.47 | 17 |
| Pb (nM) | <0.2~277 | 46.8 ± 74.7 | 16 |
| Ni (nM) | 1.7~4094 | 579 ± 1182 | 17 |

* The salinity based on relative conductivity (no unit).
** The salinity based on total dissolved solids (g/kg seawater).

Table 6
Compositions of the low temperature hydrothermal fluids near Kueishantao islet

| | Range | Mean | No. of observations |
|---|---|---|---|
| T°C | 30~65 | 50.7 ± 8.2 | 109 |
| Salinity* | 33.1~34.4 | 33.8 ± 0.35 | 110 |
| Salinity** | 31.7~34.8 | 33.2 ± 0.70 | 90 |
| pH (25 °C) | 1.84~6.96 | 3.2 ± 1.17 | 110 |
| Dissolved oxygen (μM) | <0.3~84 | 3.8 ± 12 | 108 |
| $NO_3$ (μM) | 0.02~1.18 | 0.62 ± 0.40 | 15 |
| $NO_2$ (μM) | 0.01~0.09 | 0.024 ± 0.026 | 16 |
| $NH_3$ (μM) | <0.7~179 | 14 ± 44 | 16 |
| $PO_4$ (μM) | <0.05~0.98 | 0.20 ± 0.27 | 16 |
| $SiO_2$ (μM) | 15.0~729 | 262 ± 184 | 110 |
| Chlorophyll a (μg/l) | <0.01~0.15 | 0.04 ± 0.04 | 14 |
| $CH_4$ (μM) | <0.6~283 | 46 ± 78 | 16 |
| $S^{-2}$ (μM) | <0.03~6.3 | 0.63 ± 1.6 | 16 |
| Cl (mM) | 446~561 | 519 ± 15.5 | 94 |
| $SO_4$ (mM) | 24.6~29.8 | 27.5 ± 1.00 | 94 |
| Na (mM) | 402~485 | 441 ± 15.2 | 94 |
| K (mM) | 8.79~10 | 9.40 ± 0.24 | 94 |
| Mg (mM) | 45.8~54.5 | 49.8 ± 1.52 | 94 |
| Ca (mM) | 8.62~10.6 | 9.64 ± 0.362 | 94 |
| Al (μM) | 0.29~1564 | 307 ± 375 | 107 |
| Fe (μM) | 0.031~28.9 | 7.92 ± 6.55 | 109 |
| Mn (μM) | <0.008~2.17 | 0.577 ± 0.512 | 108 |
| Cu (nM) | <0.20~26.5 | 5.25 ± 8.52 | 15 |
| Zn (nM) | <1.00~2687 | 579 ± 843 | 15 |
| Cd (nM) | <0.01~2.57 | 0.76 ± 0.86 | 15 |
| Pb (nM) | 0.4~75.1 | 15.5 ± 19.2 | 15 |
| Ni (nM) | 3.5~436 | 67.0 ± 120 | 15 |

* The salinity based on relative conductivity (no unit).
** The salinity based on total dissolved solids (g/kg seawater).

components, acidic hydrothermal fluids should show a much higher conductivity and corresponding salinity compared to salinity based on the concentration of total dissolved solids (g/kg seawater).

Therefore, in the present study, a simple experiment was performed to show the effect of acidity on salinity using seawater acidified with 1N $H_2SO_4$. The results showed a drastic increase in apparent salinity below a pH (25 °C) of 3 (Fig. 5a). When the salinity based on total dissolved solids is plotted vs. pH (Fig. 5b), the high conductivity-based salinity values in the low pH range, as shown in Fig. 5a, disappear. This is highly consistent with our earlier expectation that high conductivity-based salinities below a pH of 3 result from the high specific conductivity of $H^+$ ions. Indeed, the sample with a pH (25 °C) of 1.52 had a high conductivity-based salinity of 36.063 but a low total dissolved salt based salinity of only 30.73 (g/kg seawater). The ambient seawater salinity is 34.3 based on conductivity. Obviously, the higher conductivity-based salinity compared to the ambient seawater is due to high $H^+$ contents.

It is interesting to note that some hydrothermal fluids also have lower salinity with lower pH values which can be attributed to phase separation. The probable explanation was that we were only sampling the recondensed vapor phase, but meanwhile, the brine phase was being discharged at a deeper depth outside of our study area.

The very low total dissolved salt-based salinity for the same sample was probably caused by phase separation. The high temperature field has a slightly higher mean conductivity-based salinity ($33.9 \pm 1.3$; Table 5) than does the low temperature field ($33.8 \pm 0.39$; Table 6). Contribution of $H^+$ would make such a difference. On the other hand, the mean total dissolved solids concentration of the high temperature field is lower ($32.5 \pm 1.1$ g/kg seawater) than that of the low temperature field ($33.2 \pm 0.7$ g/kg seawater). All major ion concentrations (such as Na, K, Mg, Ca, Cl and $SO_4$, Tables 5 and 6) are also lower in the high temperature vents, perhaps because of phase separation. The high temperature field has higher concentrations of trace elements such as $SiO_2$, Fe, Mn, $CH_4$, $S^{-2}$, Cu, Cd, Pb and Ni than does the low temperature field. However, for unknown reasons, Al and Zn values are lower in the high temperature field. Dissolved oxygen (DO), $NO_3$ and $NO_2$ present in some fluid samples are a result of either contamination by ambient seawater during sampling or the mixing of ambient seawater with the hydrothermal fluids before they were discharged.

### 3.4. Temporal variations in temperature

The temperatures of the fluids reveal diurnal and bimonthly cycles (Figs. 6 and 7) although there may well be long-term variations as well. Since we have continuous records, which only cover 3 months, the discussion on this is limited. Sea level data obtained from a Seabird CTD (conductorly, temperature, depth) sensor at the same water depth but 13 m away from St. A are presented in Fig. 6. Normally, two to four hours after each high tide (high pressure), the temperature reaches a maximum, which may be indicative that the magma is shallow and that the seawater does not seep very deep beneath the seabed before the heated seawater is forced to come out due to the large buoyancy effect near the boiling point of seawater (Chen, 1981). The rapid temperature response to tides corresponds to the low $SiO_2$ and trace metal concentrations found in the hydrothermal fluids. At the water depth of St. A (13 m), a 1.2 m increase in sea level corresponds to an increase of 2 °C in the boiling point of seawater. On these grounds, the effect of buoyancy that drastically increased so much so when the hydrothermal fluid temperature approaches the boiling point is the factor that sets the limit on the

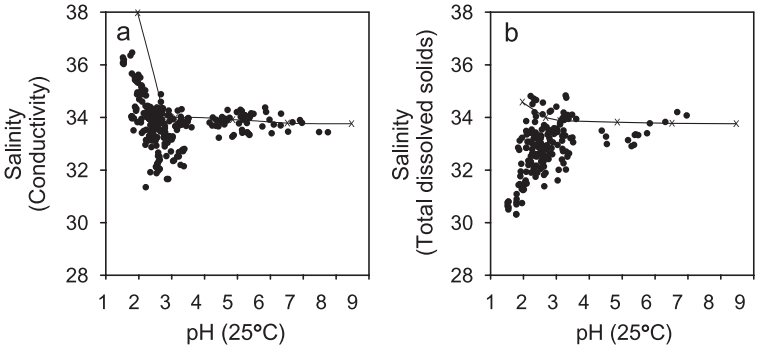


Fig. 5. (a) Conductivity-based and (b) total dissolved solids-based salinity plotted vs. the pH values (25 °C) of the hydrothermal fluids (solid circles). Crosses represent the data from the experiment where a seawater sample was artificially acidified.

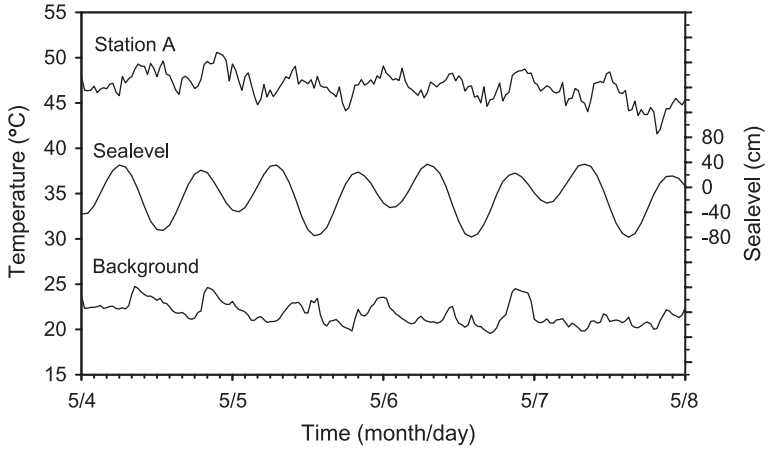


Fig. 6. Continuous temperature and sea level records at St. A between 4 and 8 May 2000. The background temperature and sea level records were taken, respectively, 1 and 13 m away from the vent.

maximum temperature that the hydrothermal fluids can attain. It follows then that under such pressure fluctuations seawater is heated 2 °C higher before it is forced to rise during high tide as opposed to during low tide some six hours later. The "background" temperature records, shown in Fig. 6, were taken only one meter away from St. A. The temperatures are about 25 °C lower, and a diurnal pattern is also evident. This station, however, was obviously affected by waters from not only St. A but also other vents nearby; hence the temperature variations.

From the 3-month records (Fig. 7), it is clear that during the monthly high tide, the temperatures of the discharge fluids are also at their highest, consistent with the above explanation. It has previously been reported in the literature that observed temperature fluctuations at hydrothermal vent sites have been known to correlate with tidal fluctuations. To cite one example, temperature fluctuations with a 12.5 h periodicity were reported for the Main Endeavour Field on the Juan de Fuca Ridge caused by several possible mechanisms, among which are tidally modulated currents on the seafloor, and tide-related, subsurface mixing of seawater with hydrothermal fluids and groundwater (Williams and Tivey, 2001). Besides these factors, higher water pressure and smaller tidal ranges in the open oceans could also minimize the effects of pressure and buoyancy. Such a phenomenon, however, has rarely been reported in the literature because most hydrothermal studies have been conducted in the deep seas for which long-term temperature records are scarce.

Temperature and sea level records at St. A alongside the path of Typhoon Bilis during the 20–24 August 2000 period are presented in Fig. 8. The presence of a diurnal temperature pattern on 20 and 21 August is

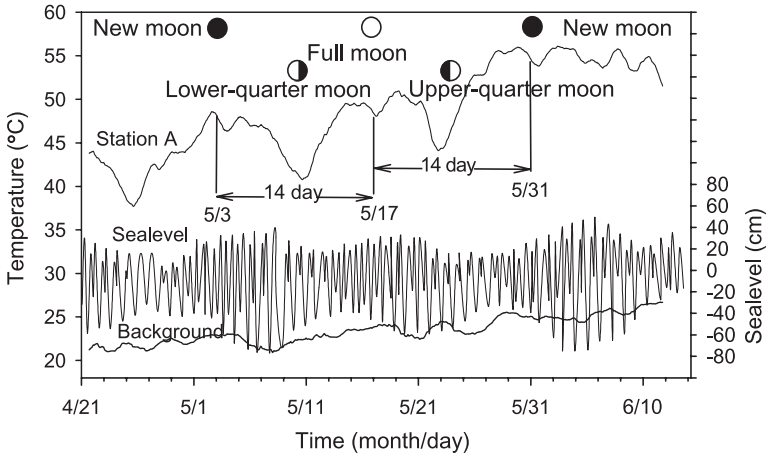


Fig. 7. Twenty-five hour moving averages of temperature and sea level at St. A between April and June 2000.

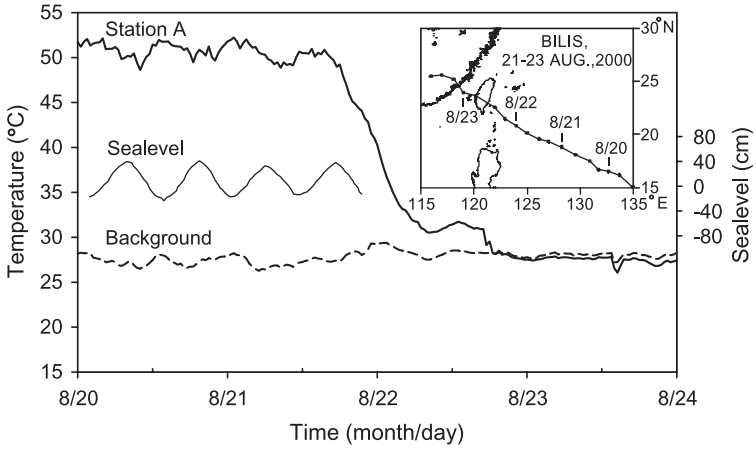


Fig. 8. Continuous temperature and sea level records at St. A between 20–24 August 2000. The insert shows the path of Typhoon Bilis.

evident, but temperatures start to decrease late on the 21st and by the 23rd of August, they plunge by about 25 °C and reach the background temperature of 27 °C. This is evidence that the disturbances caused by the typhoon either buried this vent or blocked the passage of the hydrothermal fluids and forced it to discharge elsewhere.

### 3.5. Alkalinity vs. acidity

One of the fundamental questions that has mostly remained unanswered for so long in marine chemistry is why the oceans are not more alkaline (e.g. Mackenzie and Garrels, 1966). The controversy arises from the fact that over geological timescales, the amount of dissolved calcium supplied by rivers is not large enough to account for the amount of alkalinity that is removed as $CaCO_3$ deposits on the seabed. This means that there must be an additional source of Ca or a yet unexplained sink of alkalinity (Mackenzie and Garrels, 1966; Milliman, 1993). de Villiers (1998) and de Villiers and Nelson (1999) have pointed out that a low temperature hydrothermal flux for Ca is consistent with its oceanic mass balance requirements. Worth noting, however, is that the definition of alkalinity is founded on a conservation equation for hydrogen ions, and it is zero at the $CO_2$ equivalent point which is typically in the range of pH 4 to 5. Thus, any solution with a pH below 4 is considered to have a negative alkalinity, or acidity (Morel, 1983). As most of the hydrothermal fluids found in this study are quite acidic (average pH=2.77), when combined, they reduce oceanic alkalinity by $4.5\times10^7$ mol/year. This is a very small number given that the global oceans receive $60\times10^{12}$ mol alkalinity per year, including $3\times10^{12}$ mol/year from hydrothermal vents and $10\times10^{12}$ mol/year from the continental margins (Milliman et al., 1999), or as reported by Chen (2002), an even larger shelf-generated alkalinity of $16–31\times10^{12}$ mol/year.

However, the effects of acidic hydrothermal fluid discharges may be far greater than the low acidity contributed by hydrogen ions. The reason for this is that at low pH levels, many elements that contribute to alkalinity at the seawater pH of about 8 actually end up reducing alkalinity instead. This is exemplified by the fact that at a higher pH range, each $HCO_3^-$ contributes one alkalinity because $HCO_3^-$ can combine with one $H^+$ to form $H_2CO_3$ when an acid is added. Yet at a low pH range, when a base is added, each $HCO_3^-$ can release one $H^+$ to form $CO_3^{2-}$, hence taking away one alkalinity. Morel (1983) formulated acidity as:

$$\begin{aligned}\text{Acidity} = {} & H^+ - OH^- + 2H_2CO_3 + HCO_3 + NH_4 \\ & + H_2S - S^{2-} + H_2SiO_3 + B(OH)_3 \\ & + 2H_3PO_4 + H_2PO_4^- - PO_4^{3-}.\end{aligned}$$

Unfortunately we do not have data for $H_2CO_3$, $HCO_3$ and $B(OH)_3$ in our samples. However, assume, first of all, that the hydrothermal fluids have the same total $CO_2$ and $B(OH)_3$ values as typical seawater and, secondly, that all $HCO_3^-$, $CO_3^{2-}$ and $B(OH)_4^-$ in the seawater that percolated down to form the hydrothermal fluids were converted to $H_2CO_3$ and $B(OH)_3$. Then, the alkalinity would be reduced by about 2 m mol/kg when the $CO_2$ equivalent point is reached. When multiplied by the discharge rate of about $7.6\times10^6$ ton/year of hydrothermal fluids from the study area, the total reduction in alkalinity would amount to $1.4\times10^7$ mol/year. Below the $CO_2$ equivalent point, $HCO_3^-$ and $CO_3^{2-}$ are converted to $H_2CO_3$, and each $H_2CO_3$ molecule would contribute

2 $H^+$. To sum up, there could have been an increase of $2.8 \times 10^7$ mol/year in acidity in the study area due to this process. Combining the above contributions results in $8.7 \times 10^7$ mol/year ($4.5+1.4+2.8 \times 10^7$ mol/year) in reduced alkalinity from the vents that we have sampled. As we have probably only sampled a small portion of the vents in the area and have not included the outgassed $CO_2$ from the mantle (each would take away 2 in alkalinity according to the above equation), the actual number could be several orders of magnitude higher. Noteworthy is that Resing et al. (2004) have recently estimated $CO_2$ fluxes ($1.47–2.9 \times 10^{12}$ mol/year) from the global mid-ocean ridges. This is certainly not a small amount to be neglected and deserves further study.

## 4. Conclusions

Elemental sulfur and hydrogen sulfide emitted off the coast of northeastern Taiwan originate from a cluster of shallow (<30 m depth) hydrothermal vents distributed over an area of 0.5 $km^2$. Prior to its destruction by Typhoon Bilis in August 2000, a massive 6 m high chimney with a diameter of 4 m at the base stood out among many mounds. This chimney was composed of almost pure sulfur, which was isotopically lighter than seawater and had originated from the magma degassing. The helium isotopes also suggested that the gases in the hydrothermal fluids originated from the upper mantle. The hydrothermal fluids had temperatures as high as 116 °C and values of pH (25 °C) as low as 1.52. The long-term temperature records from one vent show a very close correlation with diurnal tides suggesting rapid, shallow circulation of hydrothermal fluids.

## Acknowledgements

This work was financially supported in part by the Taiwan Power Company, the ROC National Science Council (NSC 89-2611-M-110-001) and the Pilot Project of Knowledge Innovation Project, Chinese Academy of Sciences (Grant No.KZCX34-SW-223) and the National Natural Science Foundation of China (Grant No. 40376020, 40176020). K. Brown and A. Reyes provided detailed and valuable comments which strengthened the manuscript. **[LW]**

## References

Alt, J.C., 1988. The chemistry and sulfur isotope composition of massive sulfide and associated deposits on Green Seamount, Eastern Pacific. Economic Geology 83, 1026–1033.

Arnold, M., Sheppard, S.M.F., 1981. East Pacific Rise at latitude 21°N: isotopic composition and origin of the hydrothermal sulfur. Earth and Planetary Science Letters 56, 148–156.

Blum, N., Puchelt, H., 1991. Sedimentary-hosted polymetallic massive sulfide deposits of the Kebrit and Shaban Deeps, Red Sea. Mineralium Deposita 26, 217–227.

Bluth, G.J., Ohmoto, H., 1988. Sulfide–sulfate chimneys on the East Pacific Rise, 11° and 13°N latitudes: Part II. sulfur isotopes. Canadian Mineralogist 26, 505–515.

Chen, C.H., 1996. Geological Features of Taiwan, vol. 2. Central Geological Survey, Taipei, Taiwan, p. 171.

Chen, C.H., 2000. Energy Minerals and Groundwater Resources in Taiwan, vol. 13. Geology of Taiwan, Central Geological Survey, Taipei, Taiwan, p. 218.

Chen, C.T., Gordon, L.I., 1979. Effect of the inhomogeneity of composition on conductivity of IAPSO standard seawater. Exposure 6, 1–6.

Chen, C.T.A., 1981. Geothermal system at 21°N. Science 211, 298.

Chen, C.T.A., 2002. Shelf vs. dissolution generated alkalinity above the chemical lysocline in the North Pacific. Deep-Sea Research II 49, 5365–5375.

Chen, Y.G., Wu, W.S., Chen, C.H., Liu, T.K., 2001. A date for volcanic-eruption inferred from a siltstone xenolith. Quaternary Science Reviews 20, 869–873.

Chen, C.T.A., Wang, B.J., Huang, J.F., Lou, J.Y., Kuo, F.W., Tu, Y.Y., Tsai, H.S., 2005. Investigation into extremely acidic hydrothermal fluids off Kueishantao Islet, Taiwan. Acta Oceanologica Sinica 24, 125–133.

Chiba, H., Uchiyama, N., Teagle, D.A.H., 1998. Stable isotope study of anhydrite and sulfide minerals at the TAG hydrothermal mound, Mid-Atlantic Ridge, 26°N. Proceedings of the Ocean Drilling Program, Scientific Results 158, 85–90.

de Villiers, S., 1998. Excess dissolved Ca in the deep ocean: a hydrothermal hypothesis. Earth and Planetary Science Letters 164, 627–641.

de Villiers, S., Nelson, B.K., 1999. Detection of low-temperature hydrothermal fluxes by seawater Mg and Ca anomalies. Science 285, 721–723.

Delmelle, P., Stix, J., 2000. Volcanic gases. In: Sigurdsson, P., et al. (Eds.), Encyclopedia of Volcanoes. Academic Press, pp. 803–815.

Duckworth, R., Fallick, A.E., Rickard, D., 1994. Mineralogy and sulfur isotope composition of the Middle Valley massive sulfide deposit, northern Juan de Fuca Ridge. Proceedings of the Ocean Drilling Program, Scientific Results 139, 373–385.

Fischer, T., Hilton, D.R., 2003. Tracing the sources of volcanic fluids: following Giggenbach. Geochimica et Cosmochimica Acta 67 (18), A98–A98.

Fischer, T.P., Arehart, G.B., Sturchio, N.C., Williams, S.N., 1996. The relationship between fumarole gas composition and eruptive activity at Galeras volcano, Colombia. Geology 24 (6), 531–534.

Gamo, T., Okamura, K., Charlou, J.L., Urabe, T., Auzende, J., Ishibashi, J., Shitashima, K., Chiba, H., 1997. Acidic and sulfate-rich hydrothermal fluids from the Manus back-arc basin, Papua New Guinea. Geology 25, 139–142.

Gemmell, J.B., Sharpe, R., 1998. Detailed sulfur-isotope investigation of the TAG hydrothermal mound and stockwork zone, 26°N, Mid-Atlantic Ridge. Proceedings of the Ocean Drilling Program, Scientific Results 158, 71–84.

Giggenbach, W.F., 1975. A simple method for the collection and analysis of volcanic gas samples. Bulletin of Volcanology 39, 132–145.

Giggenbach, W.F., Matsuo, S., 1991. Evaluation of results from second and third IAVCEI field workshop on volcanic gases, Mt. Usu, Japan and White Island, New Zealand. Applied Geochemistry 6, 125–141.

Giggenbach, W.F., Tedesco, D., Sulistiyo, Y., Caprai, A., Cioni, R., Favara, R., Fischer, T.P., Hirabayashi, J.-I, Korzhinsky, M., Martini, M., Menyailov, I., Shinohara, H., 2001. Evaluation of results from the fourth and fifth IAVCEI field workshops on volcanic gases, Vulcano island, Italy and Java, Indonesia. Journal of Volcanology and Geothermal Research 108, 157–172.

Goodfellow, W.D., Franklin, J.M., 1993. Geology, mineralogy, and chemistry of sediment-hosted clastic massive sulfides in shallow cores, Middle Valley, northern Juan de Fuca Ridge. Economic Geology 88, 2037–2068.

Halbach, P., Nakamura, K., Washner, M., Lange, J., Sakai, H., Kaselitz, L., Hansen, R.D., Yamano, M., Post, J., Prause, B., Seifert, R., Michaelis, W., Teichmann, F., Kinoshita, M., Marten, A., Ishibashi, J., Czerwinski, S., Blum, N., 1989. Probable modern analogue of Kuroko-type massive sulphide deposits in the Okinawa trough back-arc basin. Nature 338, 496–499.

Hannington, M.D., Scott, S.D., 1988. Mineralogy and geochemistry of a hydrothermal silica–sulfide–sulfate spire in the Caldera of Axial Seamount, Juan de Fuca Ridge. Canadian Mineralogist 26, 603–625.

Hekinian, R., Fevrier, M., Bischoff, J.L., Picot, P., Shanks III, W.C., 1980. Sulfide deposits from the East Pacific Rise, 21°N. Science 207, 1433–1444.

Herzig, P.M., Hannington, M.D., Arribas Jr., A., 1998a. Sulfur isotopic composition of hydrothermal precipitates from the Lau backarc: implications for magmatic contributions to seafloor hydrothermal systems. Mineralium Deposita 33, 226–237.

Herzig, P.M., Petersen, S., Hannington, M.D., 1998b. Geochemistry and sulfur-isotopic composition of the TAG hydrothermal mound, Mid-Atlantic Ridge, 26°N. Proceedings of the Ocean Drilling Program, Scientific Results 158, 47–70.

Kase, K., Yamamoto, M., Shibata, T., 1990. Copper-rich sulfide deposit near 23°N, Mid-Atlantic Ridge, chemical composition, mineral chemistry and sulfur isotopes. Proceedings of the Ocean Drilling Program, Scientific Results 106/109, 163–177.

Kerridge, J., Haymon, R.M., Kastner, M., 1983. Sulfur isotope systematics at the 21°N site, East Pacific Rise. Earth and Planetary Science Letters 66, 91–100.

Knott, R., Fouquet, Y., Honnorez, J., Petersen, S., Bohn, M., 1998. Petrology of hydrothermal mineralization. A vertical section through the TAG mound. Proceedings of the Ocean Drilling Program, Scientific Results 158, 5–26.

Kusakabe, M., Mayeda, S., Nakamara, E., 1990. S, O and Sr isotope systematics of active vent materials from the Mariana backarc basin spreading axis at 18°N. Earth and Planetary Science Letters 100, 275–282.

Koski, R.A., Shanks III, W.C., Bohrson, W.A., Oscarson, R.L., 1988. The composition of massive sulfide deposits from the sediment-covered floor of Escanaba Trough, Gorda Ridge, implications for depositional processes. Canadian Mineralogist 26, 655–673.

Koski, R.A., Lonsdale, P.F., Shanks III, W.C., Berndt, M.E., Howe, S.S., 1985. Mineralogy and geochemistry of a sediment-hosted hydrothermal sulfide deposit from the southern trough of Guaymas Basin, Gulf of California. Journal of Geophysical Research 90, 6695–6707.

Lee, C.S., Shor Jr., G.G., Bibce, L.D., Lu, R.S., Hilde, T.W.C., 1980. Okinawa Trough: origin of a back-arc basin. Marine Geology 35, 219–241.

Lee, H.F., Yang, T.F., 2005. Fumarolic gas compositions of Tatun Volcano Group, northern Taiwan. TAO (revised).

Lee, H.F., Yang, T.F., Lan, T.F., 2005. Fumarolic gas compositions of Tatun Volcano Group, northern Taiwan. Terrestrial, Atmospheric and Oceanic Sciences (revised).

Mackenzie, F.T., Garrels, R.M., 1966. Chemical mass balance between rivers and oceans. American Journal of Science 264, 507–525.

Marumo, K., Hattori, K., 1999. Seafloor hydrothermal clay alteration at Jade in the back-arc Okinawa Trough: Mineralogy, geochemistry and isotope characteristics. Geochimica et Cosmochimica Acta 63, 2785–2804.

Milliman, J.D., 1993. Production and accumulation of calcium carbonate in the ocean: budget. Global Biogeochemical Cycles 7, 927–957.

Milliman, J.D., Troy, P.J., Balch, W.M., Adams, A.K., Li, Y.H., Mackenzie, F.T., 1999. Biologically mediated dissolution of calcium carbonate above the chemical lysocline? Deep-Sea Research I 46, 1653–1669.

Morel, F.M.M., 1983. Principles of Aquatic Chemistry. Wiley-Interscience, New York, p. 446.

Peter, J.M., Shanks III, W.C., 1992. Sulfur, carbon, and oxygen isotope variations in submarine hydrothermal deposits of Guaymas Basin, Gulf of California. Geochimica et Cosmochimica Acta 56, 2025–2040.

Poreda, R., Craig, H., 1989. Helium isotope ratios in Circum-Pacific volcanic arcs. Nature 338, 473–478.

Rees, C.E., Jenkins, W.J., Monster, J., 1978. The sulfur isotopic composition of ocean water sulfate. Geochimica et Cosmochimica Acta 42, 377–381.

Resing, J.A., Lupton, J.E., Feely, R.A., Lilley, M.D., 2004. $CO_2$ and $^3He$ in hydrothermal plumes: implications for mid-ocean ridge $CO_2$ flux. Earth and Planetary Science Letters 226, 449–464.

Sakai, H., DesMarais, D.J., Ueda, A., Moore, J.G., 1984. Concentrations and isotope ratios of carbon, nitrogen and sulfur in ocean-floor basalts. Geochimica et Cosmochimica Acta 48, 2433–2441.

Shanks III, W.C., Niemitz, J., 1982. Sulfur isotope studies of hydrothermal anhydrite and pyrite. In Initial Reports of the Deep Sea Drilling Project 64, 1137–1142.

Shanks III, W.C., Seyfried Jr., W.E., 1987. Stable isotope studies of vent fluids and chimney minerals, southern Juan de Fuca Ridge, sodium metasomatism and seawater sulfate reduction. Journal of Geophysical Research 92, 11387–11399.

Stuart, F.M., Duckworth, R., Turner, G., Schofield, P., 1994. Helium and sulfur isotopes in sulfides from the Middle Valley, northern Juan de Fuca Ridge. Proceedings of the Ocean Drilling Program, Scientific Results 139, 387–392.

Taran, Y.A., Fischer, T.P., Cienfuegos, E., Morales, P., 2002. Geochemistry of hydrothermal fluids from an intraplate ocean island: Everman volcano, Socorro Island, Mexico. Chemical Geology 188 (1–2), 51–63.

Ueda, A., Sakai, H., 1984. Sulfur isotope study of Quaternary volcanic rocks from the Japanese island arc. Geochimica et Cosmochimica Acta 48, 1837–1848.

Wang, C.S., Huang, C.-P., Ke, L.-Y., Chien, W.-J., Hsu, S.-K., Shyu, C.-T., Cheng, W.-B., Lee, C.-S., Teng, L.S., 2002. Formation of the Taiwan Island as a solitary wave along the Eurasian continental plate margin: magnetic and seismological evidence. Terrestrial, Atmospheric and Oceanic Sciences 13, 339–354.

Williams III, A.J., Tivey, M.K., 2001. Tidal currents at hydrothermal vents, Juan de Fuca Ridge. Sea Technology 62–64 (June, 2001).

Woodhead, J.D., Harmon, R.S., Fraser, D.G., 1987. O, S, Sr and Pb isotope variations in volcanic rocks from the northern Mariana islands, implications for crustal recycling in intra-oceanic arcs. Earth and Planetary Science Letters 83, 39–52.

Woodruff, L.G., Shanks, W.C., 1988. Sulfur isotope study of chimney minerals and hydrothermal fluids from 21°N, East Pacific Rise: hydrothermal sulfur sources and disequilibrium sulfate reduction. Journal of Geophysical Research 93, 4562–4572.

Yang, T.F., 2000. The helium isotopic ratios of fumaroles from Tatun Volcano Group of Yangmingshan National Park, N. Taiwan. Journal of National Park 10 (1), 73–94 (in Chinese with English abstract).

Yang, T.F., Lee, C.S., Chen, C.T.A., 2005. Gas compositions and helium isotopic ratios of fluid samples around Kueishantao, NE offshore Taiwan and its tectonic implications. Geochemical Journal (in preparation).

Yang, T.F., Chen, C.-H., Tien, R.L., Song, S.R., Liu, T.K., 2003. Remnant magmatic activity in the Coastal Rang of East Taiwan after arc-continent collision: fission-track date and $^{3}He/^{4}He$ ratio evidence. Radiation Measurements 36, 343–349.

Zeng, Z.G., Jiang, F.Q., Zhai, S.K., Qin, Y.S., Hou, Z.Q., 2000a. Sulfur isotopic composition of seafloor hydrothermal sediment from the Jade hydrothermal field in the central Okinawa Trough and its geological significance. Acta Oceanologica Sinica 22, 74–82 (in Chinese with English abstract).

Zeng, Z.G., Qin, Y.S., Zhao, Y.Y., Zhai, S.K., 2000b. Sulfur isotopic composition of seafloor surface hydrothermal sediments in TAG hydrothermal field of Mid-Atlantic Ridge and its geological significance. Oceanologia et Limnologia Sinica 31, 518–529 (in Chinese with English abstract).

Zheng, Y.F., Fu, B., Zhang, X.H., 1996. Effects of magma degassing on the carbon and sulfur isotope compositions of igneous rocks. Scientia Geologica Sinica 31, 43–53 (in Chinese with English abstract).

Zierenberg, R.A., 1994. Sulfur content of sediment and sulfur isotope values of sulfide and sulfate minerals from Middle Valley. Proceedings of the Ocean Drilling Program, Scientific Results 139, 739–748.

Zierenberg, R.A., Shanks III, W.C., 1988. Isotopic studies of epigenetic features in metalliferous sediment, Atlantis II Deep, Red Sea. Canadian Mineralogist 26, 737–753.

Zierenberg, R.A., Shanks III, W.C., Bischoff, J., 1984. Massive sulfide deposits at 21°N EPR, chemical composition, stable isotopes, and phase equilibria. Geological Society of America Bulletin 95, 922–929.

Zierenberg, R.A., Koski, R.A., Morton, J.L., Bouse, R.M., Shanks III, W.C., 1993. Genesis of massive sulfide deposits on a sediment-covered spreading center, Escanaba Trough, Southern Gorda Ridge. Economic Geology 88, 2069–2098.